PHYSICAL REVIEW E **71**, 025401(R) (2005)

Laser-driven hard-x-ray generation based on ultrafast selected energy x-ray absorption spectroscopy measurements of Ni compounds

Fang Shan, Josh D. Carter, Vicky Ng, and Ting Guo*
Department of Chemistry, University of California, One Shields Avenue, Davis, California 95616, USA
(Received 6 June 2004; revised manuscript received 20 December 2004; published 4 February 2005)

Three Ni compounds were studied by ultrafast selected energy x-ray absorption spectroscopy using a laser-driven electron x-ray source with a tungsten target. The measured *K* edges of these Ni compounds using this self-referencing method were made identical to those measured with synchrotron x-ray sources. This enabled us to determine the absolute peak positions of tungsten $L\alpha_1$ and $L\alpha_2$ emitted from this source to be within 1 eV of those from the neutral tungsten atoms, which strongly suggested that the x rays were emitted from high energy electrons interacting with tungsten atoms in the solid target. This is the best evidence to date that directly supports the cold atom x-ray generation theory.

DOI: 10.1103/PhysRevE.71.025401 PACS number(s): 52.38.−r

I. INTRODUCTION

Ultrafast characteristic and continuum hard x rays (a few keV to a hundred keV) can be generated by focusing an intense laser beam onto a solid or liquid target [1–4], and have been used in ultrafast x-ray absorption and diffraction experiments [5–8]. In order to make ultrafast x-ray sources more suitable for these applications, many efforts have been spent on improving these sources.

Two popular models for the x-ray generation mechanisms of these ultrafast hard x-ray pulses have been proposed. One school of thought regards that those x rays are generated through a two-step process [3]. In the first step, intense ultrafast laser pulses interact with only the electrons in a dilute plasma of near critical density n_c (less than the solid density) for the input light. Strong energy coupling between the laser light and the electrons ensues, and the electrons are greatly accelerated. Because of the low density of the plasma, the yield of hard x rays generated from the interaction between the accelerated electrons and the plasma or from the recombination of the highly ionized ions in the plasma is low. In the second half of the x-ray production process, this burst of accelerated electrons interact with the cold atoms in the solid target nearby to produce x rays. As a result, intense characteristic and bremsstrahlung hard x-ray pulses are produced. This model and its variations are generally accepted when the x rays are in the multi-keV or higher region. In fact, the second half of this model is almost identical to that of bombarding a solid target with a continuous, monoenergetic electron beam in common x-ray tubes, except that the electrons are not monoenergetic in the former case. Nonetheless, the characteristic emission lines from such laser-driven x-ray sources should resemble closely those from the cold atoms in x-ray tubes. We term this the cold atom theory for ultrafast hard x-ray generation. Although low resolution and calibrated ($>$100 eV), or high resolution and noncalibrated ($<$1 eV), characteristic x-ray emission data were obtained; calibrated and high spectral resolution experimental data have not been available to directly prove such a theory [3,9–13]. In some other cases, high resolution spectra calibrated with concomitant characteristic hard x-rays from gas targets were obtained [14,15]. However, those characteristic lines themselves were not calibrated.

A competing model that has been widely used to explain low energy x-ray generation (sub 1 keV) suggests that x rays are produced due to the recombination (filling of the inner-shell vacancies, but not limited to the *K*-shell vacancies) of highly ionized ions in a thermal plasma produced by an intense laser field interacting with a *solid density* plasma. In those cases, bound-bound transitions in the ions result in the x-ray generation [4,16]. Stark shift and the broadening of line emission, and ionization threshold depression are severe during the evolution of the plasma, generating bursts of broadband soft x rays [17–20]. The solid density plasmas can cool rapidly due to the high rate of heat exchange with the rest of the solid target. Many studies on the gas-phase materials have also yielded similar results with longer pulse durations [21]. We call this model the hot plasma theory. Both mechanisms are capable of generating ultrafast, subpicosecond x-ray pulses, depending on the experimental conditions.

In order to further identify the mechanisms of hard x-ray generation, high-resolution and calibrated spectra of the emitted x rays are needed. In this paper, we wish to report the results obtained with a method developed in our laboratory, ultrafast selected energy x-ray absorption spectroscopy (USEXAS). This method uses characteristic x-ray radiation to obtain x-ray absorption spectra [22,23]. The self-referencing feature made possible by the inclusion of the characteristic lines *and* the absorption edges of known compounds in the same x-ray absorption spectra allows us to determine the peak positions of characteristic emission lines in the hard x-ray region with high energy resolution. This enables us to effectively differentiate the two x-ray generation mechanisms.

II. EXPERIMENT

Parts of the laser and x-ray systems were described elsewhere [24]. The overall setup is shown in Fig. 1. In brief,

*Fax: 530-752-8995; Electronic address: tguo@ucdavis.edu

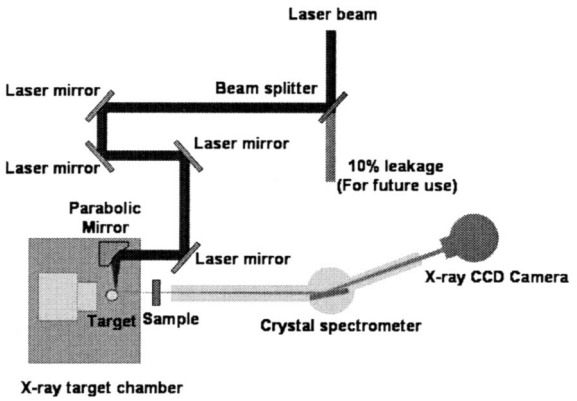

FIG. 1. Experimental layout for x-ray generation and detection.

90% of a 55-mJ/pulse at a 50-Hz repetition rate laser beam was directed into an x-ray chamber. The beam, through a Mylar protection film, was focused onto a moving Cu (wire) or W (rod) target by a parabolic mirror (Janos A8037-274). For the W target, the rod moved down, driven by a step motor-driven linear stage and simultaneously rotated-driven by a second step motor. The lateral jittering motion of the rod was confined to <12 μm (end-to-end) by three actuators (Newport). GaAs(111) or Si(111) single crystals were used to diffract the x rays into a liguid-nitrogen-cooled, deep depletion charged-coupled device (CCD) detector (Roper Scientific, PI-LCX 576).

3-μm Ni foils (Goodfellow) and NiO powders (99%, Aldrich) were purchased and were used without further treatment. Nickel tetraphenylporphyrin (NiTPP) powder (95%) was purchased from Mid-Century Chemicals. All samples were in the form of thin films, and were prepared using the common ir pellet preparation method. The samples were then covered with Kapton thin films (SPEX) and mounted on a half-inch iris. The equivalent thicknesses of Ni in the NiO and NiTPP films to the Ni bulk films were between 3 and 4 μm, deduced from the x-ray measurements.

Absorption data was processed *in situ* using a Matlab program. Each diffraction data file acquired by the x-ray CCD contained a two-dimensional matrix. The column position corresponded to the x-ray energy. Without the samples in the x-ray beam path, the column positions of the two diffraction peaks shown in the diffraction patterns from the tungsten target were assigned to the theoretical values of W $L\alpha_1$ at 8.3976 keV and W $L\alpha_2$ at 8.3352 keV, respectively [25]. Based on these two positions, the rest of the columns were assigned to their corresponding energies based on linear interpolation and extrapolation. The counts along the row were then added to obtain the total x-ray intensity (I_0). A similar process was used to obtain the x-ray intensity profiles (I) with the samples, except that the energy calibration method of the diffraction profiles from I_0 was used. The absorbance was then calculated from $A=\mu L=-\ln(I/I_0)$ as a function of energy, in which μ and L are absorption coefficient and sample thickness.

Synchrotron data was obtained at beamline 4-1 at the Stanford Synchrotron Radiation Laboratory (SSRL). NiO solution in deionized water and Ni foil were measured in the fluorescence mode. The data were processed with EXAFSPAK [26]. The data were calibrated using a standard Ni foil at SSRL. NiTPP data were adopted from Chen *et al.* [27].

III. RESULTS

We measured the direct and diffracted x rays from the tungsten x-ray target using three single crystals to verify that whether or not those measurements were affected by these crystals. The results showed that the yields measured in the direct and diffracted modes were similar, although the diffraction efficiency of Si(111) single crystals (Czochralski-grown, undoped; Virginia Semiconductor and Frozen zone grown, B doped, Valley Design) was 50% of that of the GaAs crystal (Virginia Semiconductor). The GaAs produced lower resolution USEXAS spectra. When all the x-rays detected by the detector were counted, the highest total flux of $L\alpha_1$ and $L\alpha_1$ from W was 6×10^{10} photons/$(4\pi$ Sr s).

We also measured x rays from the Cu wire target. Under optimal conditions, the intensity of the diffracted Cu x rays detected with the CCD was similar to those measured earlier

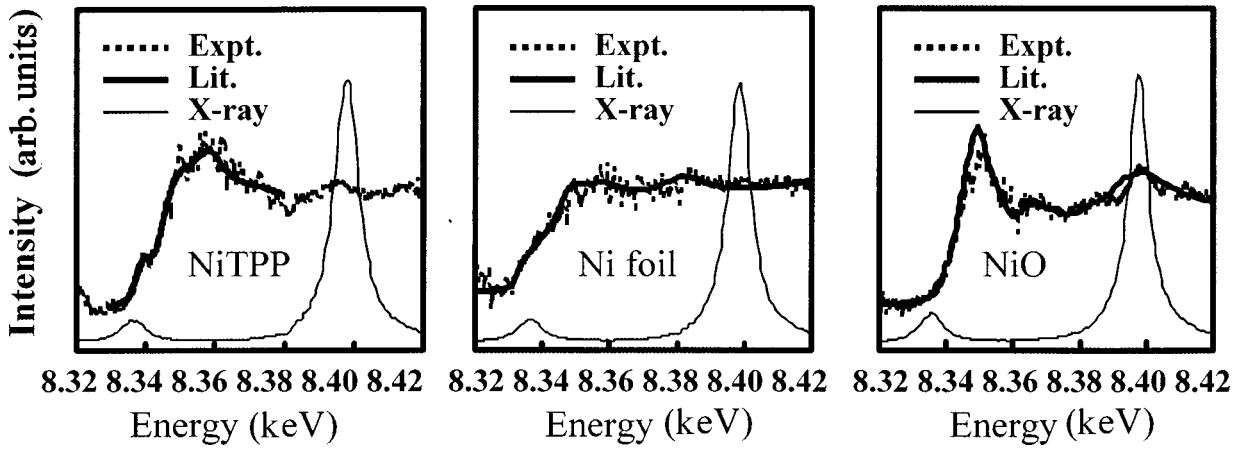

FIG. 2. USEXAS data on NiTPP, Ni, and NiO. The experimental data (dotted), the synchrotron data (dark solid), and the tungsten $L\alpha_1$ and $L\alpha_2$ lines are shown for each sample. The NiTPP synchrotron data were adopted from Chen *et al.* [27].

TABLE I. Results of x-ray absorption edges for Ni, NiO, and NiTPP measured with USEXAS and synchrotron (in eV). The theoretical spectral positions for W $L\alpha_1$ and $L\alpha_2$ used to obtained the USEXAS results are also listed.

	Ni	NiO	NiTPP
USEXAS	8330.7(+1)	8337.8(+0.4)	8335.0(−0.5)
Synchrotron	8329.7	8337.4	8335.5
Theoretical $L\alpha_1$	8397.6	Theoretical $L\alpha_2$	8335.2

[3,24]. The highest flux for Cu $K\alpha_1$ and $K\alpha_2$ was 5×10^{10} photons/$(4\pi$ Sr s), and the total energy conversion efficiency was 5×10^{-5} after correction of other losses. The yield was calculated with corrections of air absorption and detector efficiency. The peak laser intensities were $\sim2\times10^{17}$ W/cm^2, and the pulse duration was $\sim$400–600 fs (after adjustment of the grating separation to favor hard x-ray generation). The smallest focal spot size was used, although the current parabola produced a relatively large spot size of 10-μm in diameter. We observed a similar yield dependency on the grating separation to that reported earlier: the yield increased when the pulse was lengthened from the shortest value, and decreased quickly after the pulse became longer than 1 ps [24]. We also adjusted the target position to vary the laser focal spot size. The results were similar to the grating separation adjustments.

The measurements of Ni *K* edges with the W target using the Si(111) crystal spectrometer are shown in Fig. 2 (dotted lines). The USEXAS results of all three Ni compounds are shown. The synchrotron data (solid lines) are also presented, and that of NiTPP was adopted from Chen *et al.* [27]. Also shown in Fig. 2 are the x-ray emission spectra of tungsten $L\alpha_1$ and $L\alpha_2$. All the important features associated with these three samples were reproduced in our measurements, and the Ni pre-edge in NiTPP is clearly visible [27]. Table I presents the *K* absorption edges (using the first inflection point) of the three Ni compounds measured with USEXAS. Since our data were processed based on the theoretical peak positions of $L\alpha_1$ and $L\alpha_2$ from cold tungsten atoms, the measured absorption edges were identical to those of the same samples measured with the synchrotron indicates that the peak positions of the emitted hard x rays are identical to that of the cold tungsten atoms. In Table I, the differences between the measured values using USEXAS and those with the synchrotron are shown in the parentheses, and they are all within 1 eV from the processed data using the theoretical peak positions of $L\alpha_1$ (right peak in each panel) and $L\alpha_2$ mentioned earlier. Since the 1-eV values are close to the energy resolution of the Si(111) crystal diffractometer, we consider that these two peak positions are the true values for the emitted hard x rays within the experimental uncertainty.

IV. DISCUSSION

Other measurements on the tungsten *L* lines were made, although the spectral resolution in those measurements was low. Hironaka *et al.* measured 8.51 ± 0.12 keV [10]. Fujimoto *et al.* measured with a 36-eV-shift based on the CCD resolution [9]. As mentioned above, the line emission of other elements was measured, but none of these data were calibrated. Previously, high resolution data available without spectral position calibration were the results of the measurement of vanadium *K* lines using a Von Hamos crystal spectrometer. The measured positions were 6–8 eV lower than the theoretical values [28].

Because of the high energy resolution ($\sim$1 eV) for the absorption edge data reported here and the derived peak positions of the W $L\alpha_1$ and $L\alpha_2$, we consider that this is the clearest indication that the x rays are generated as the result of electrons interacting with the neutral atoms or low oxidation state ions in the W target, and not produced from highly ionized ions, as the Stark shifts and broadening will alter the emission profiles.

It is worth pointing out that the $L\alpha$ lines, which originate from transitions between L_{III} and M_{IV} or M_{V} levels, are less susceptible to the chemical environmental changes than the edges themselves. Further studies are needed to characterize transitions between *L* and *N* or even *O* levels to more sensitively detect the changes to those edges in different chemical environments. Nonetheless, our measurements shown here provide high resolution data to support that hard x-ray emission is produced from neutral or low oxidation state atoms in the target.

V. CONCLUSION

Using the self-referencing feature made possible by the presence of both the characteristic lines and the absorption edges of known compounds in the same x-ray absorption spectrum in USEXAS, we have determined the peak position of characteristic emission lines in the hard x-ray region with high energy resolution. This allows us to select the cold atom theory as the x-ray generation mechanism.

ACKNOWLEDGMENTS

We thank the National Science Foundation, Grant No. CHE 0135132, and the Camille and Dreyfus Foundation and UC Davis for their financial support. We thank the excellent staff at Stanford Synchrotron Radiation Laboratory (SSRL) for experimental support. We are grateful to DOE for support of the facility.

[1] J. C. Kieffer, M. Chaker, J. P. Matte, H. Pepin, C. Y. Cote, Y. Beaudoin, T. W. Johnston, C. Y. Chien, S. Coe, G. Mourou, and O. Peyrusse, Phys. Fluids B **5**, 2676 (1993).

[2] A. Rousse, P. Audebert, J. P. Geindre, F. Fallies, J. C. Gauthier, A. Mysyrowicz, G. Grillon, and A. Antonetti, Phys. Rev. E **50**, 2200 (1994).

[3] T. Guo, C. Spielmann, B. C. Walker, and C. P. J. Barty, Rev. Sci. Instrum. **72**, 41 (2001).

[4] M. M. Murnane, H. C. Kapteyn, M. D. Rosen, and R. W. Falcone, Science **251**, 531 (1991).

[5] T. Guo, C. Rose-Petruck, R. Jimenez, F. Raski, J. A. Squier, B. C. Walker, K. R. Wilson, and J. P. C. Barty, Proc. SPIE **3157**, 84 (1997).

[6] C. Rose-Petruck, R. Jimenez, T. Guo, A. Cavalleri, C. W. Siders, F. Raksi, J. A. Squier, B. C. Walker, K. R. Wilson, and C. P. J. Barty, Nature (London) **398**, 310 (1999).

[7] F. Raksi, K. R. Wilson, Z. M. Jiang, A. Ikhlef, C. Y. Cote, and J. C. Kieffer, J. Chem. Phys. **104**, 6066 (1996).

[8] I. V. Tomov and P. M. Rentzepis, Chem. Phys. **299**, 203 (2004).

[9] Y. Fujimoto, Y. Hironaka, K. G. Nakamura, K. Kondo, M. Yoshida, M. Ohtani, and H. Tsunemi, Jpn. J. Appl. Phys., Part 1 **38**, 6754 (1999).

[10] Y. Hironaka, T. Inoue, Y. Fujimoto, K. G. Nakamura, K. Kondo, and M. Yoshida, Jpn. J. Appl. Phys., Part 2 **38**, L242 (1999).

[11] L. M. Chen, P. Forget, R. Toth, J. C. Kieffer, A. Krol, C. C. Chamberlain, B. X. Hou, J. Nees, and G. Mourou, Rev. Sci. Instrum. **74**, 5035 (2003).

[12] M. Hagedorn, J. Kutzner, G. Tsilimis, and H. Zacharias, Appl. Phys. B: Lasers Opt. **77**, 49 (2003).

[13] A. Thoss, M. Richardson, G. Korn, M. Faubel, H. Stiel, U. Vogt, and T. Elsaesser, J. Opt. Soc. Am. B **20**, 224 (2003).

[14] A. I. Magunov, A. Y. Faenov, I. Y. Skobelev, T. A. Pikuz, E. Biemont, P. Quinet, F. Blasco, C. Bonte, F. Dorchies, T. Caillaud, F. Salin, and C. Stenz, J. Exp. Theor. Phys. **95**, 998 (2002).

[15] A. Y. Faenov, I. Y. Skobelev, S. A. Pikuz, G. A. Kyrala, R. D. Fulton, J. Abdallah, and D. P. Kilcrease, Phys. Rev. A **51**, 3529 (1995).

[16] J. C. Kieffer, C. Y. Chien, F. Dorchies, P. Forget, P. Gallant, Z. M. Jiang, and H. Pepin, C. R. Acad. Sci., Ser IV: Phys., Astrophys. **1**, 297 (2000).

[17] J. Workman, A. Maksimchuk, X. Liu, U. Ellenberger, J. S. Coe, C. Y. Chien, and D. Umstadter, Phys. Rev. Lett. **75**, 2324 (1995).

[18] W. H. Goldstein, A. Zigler, P. G. Burkhalter, D. J. Nagel, A. Barshalom, J. Oreg, T. S. Luk, A. McPherson, and C. K. Rhodes, Phys. Rev. A **47**, 4349 (1993).

[19] U. Teubner, C. Wulker, W. Theobald, and E. Forster, Phys. Plasmas **2**, 972 (1995).

[20] C. Y. Chien, J. S. Coe, G. Mourou, J. C. Kieffer, M. Chaker, Y. Beaudoin, O. Peyrusse, and D. Gilles, Opt. Lett. **18**, 1535 (1993).

[21] B. K. F. Young, A. L. Osterheld, D. F. Price, R. Shepherd, R. E. Stewart, A. Y. Faenov, A. I. Magunov, T. A. Pikuz, I. Y. Skobelev, F. Flora, S. Bollanti, P. Di Lazzaro, T. Letardi, A. Grilli, L. Palladino, A. Reale, A. Scafati, and L. Reale, Rev. Sci. Instrum. **69**, 4049 (1998).

[22] G. Cheng, F. Shan, A. Freyer, and T. Guo, *Applications of X rays Generated from Lasers and Other Bright Sources II* (SPIE, San Diego, 2001), p. 1.

[23] F. Shan, J. D. Carter, V. Ng, and T. Guo, Proc. SPIE **5340**, 23 (2004).

[24] G. J. Cheng, F. Shan, A. Freyer, and T. Guo, Appl. Opt. **41**, 5148 (2002).

[25] J. A. Bearden, Rev. Mod. Phys. **39**, 78 (1967).

[26] G. N. George and I. J. Pickering, SSRL, Stanford, 1995 (unpublished).

[27] L. X. Chen, W. J. H. Jager, G. Jennings, D. J. Gosztola, A. Munkholm, and J. P. Hessler, Science **292**, 262 (2001).

[28] Z. Jiang, J. C. Kieffer, J. P. Matte, M. Chaker, O. Peyrusse, D. Gilles, G. Korn, A. Maksimchuk, S. Coe, and G. Mourou, Phys. Plasmas **2**, 1702 (1995).